RSC Advances

ROYAL SOCIETY OF CHEMISTRY

www.rsc.org/advances

Use of CS-PAA nanoparticle as alternative of metal oxide nanoparticle and its effect on fouling mitigation of PSF ultrafiltration membrane

M. K. Sinha and M. K. Purkait*

Department of Chemical Engineering

Indian Institute of Technology Guwahati

Guwahati - 781039, Assam, India

* Corresponding author

Tel: + 91 - 361 - 2582262

Fax: +91 - 361 - 2582291

E. Mail: mihir@iitg.ernet.in

Abstract

This study deals with the synthesis and characterization of cross linked chitosan polyacrylic acid (CS-PAA) nanoparticle. Phase inversion method was used to prepare the blended polysulfone (PSF) membranes with CS-PAA nanoparticle. Field emission scanning electron microscope (FESEM) and attenuated total reflectance-Fourier transform infrared spectroscopy (ATR-FTIR) measurements were performed to confirm the presence and dispersion of the CS-PAA nanoparticles in the blended membranes. Modified membranes exhibited superior pore size, pure water flux, hydraulic permeability and fouling resistance compared to the plain membrane. Morphology of the modified membranes was changed noticeably with more quantity of nanoparticle. Hydrophilicity and fouling resistance behaviour of the fabricated membranes were evaluated in terms of water contact angle and BSA adsorption, respectively. Hydraulic permeability was also determined and it improved from 0.146 L/m^2h kPa to 0.265 L/m^2h kPa for modified membrane compared to plain membrane. Fouling resistance performance of modified membrane was estimated by ultrafiltration (UF) of 1000 ppm Bovine serum albumin (BSA) solution. BSA flux was improved from 8.3 to 24.3 L/m^2h for modified membranes. Modified membrane reached a maximum flux recovery ratio of around 88 % after BSA UF experiment compared to 42 % flux recovery ratio of plain membrane.

Keywords: Polymeric nanoparticle; hydrophilic; fouling resistance; chitosan; ultrafiltration.

1. Introduction

Ultrafiltration membranes are widely used for medical, biological and pharmaceutical application as well as in food and beverage industry for separation of fermentation product with high yield and purity.[1-3] The reason of wide spread use of these membranes are easy operation, low energy expenditure, non requirement of phase change and compact design. Ultrafiltration membranes are mainly prepared by polymer material by phase inversion method. Among different polymer materials, polysulfone/polyether sulfone (PES) is most preferred material due to their resistance to chemical and chlorine, good physicochemical stability, wide operating range of pH.[4] The other most important reason is the solubility of PSF since it allows to co-dissolve other polymeric materials, which makes it ideal material for fabrication of ultrafiltration membranes by phase inversion method. In addition, durability of PSF membranes due to their good mechanical and thermal stability makes them ideal choice for general filtration purpose.[5] However; hydrophobic property of PSF/PES membranes is their major disadvantage. Due to the hydrophobicity, PSF/ PES membranes are susceptible to deposition and adsorption of foulants like fatty acid, protein and organic matter onto the membrane surface or inside the pores, this amplify the hydraulic resistance and reduce the flux through membrane.[6]

Several methods have been developed to overcome this problem. Mainly four methods are used for the modification PSF ultrafiltration membrane. First is pre functionalization of PSF (before membrane preparation) by tailoring the hydrophilic functional group to PSF chain like carboxyl, sulfonyl hydroxide and amine.[7-9] Second is modification of membrane by surface grafting via redox initiated grafting, UV induced grafting, plasma treatment.[10] Third method is modification of PSF membrane by thin film coating.[11] Fourth method is blending of additive in membrane casting solution. It is most easy

and preferred method for the modification of PSF membrane. Various materials like surfactant, water soluble polymer, hydrophilic polymer and charged polymer have been blended with casting solution for the modification purpose.[12-15] Besides blending different type of polymer materials, recently a lot of attention has been given to the blending of nanoparticles. The nanoparticles mixed into the polymeric membrane casting solution mainly include TiO_2, SiO_2, $Mg(OH)_2$, Al_2O_3, ZnO, carbon nanotubes, boehmite nanoparticles.

Razmjou et al.[16] used modified and unmodified TiO_2 nanoparticle for the modification of PES membrane by blending it in PES membrane casting solution. They found that modified TiO_2 could produce membrane with higher hydrophilicity and better permeation performance. Although, the maximum flux and flux recovery ratio was obtained when 2 wt. % of modified TiO_2 nanoparticle was used. Unmodified TiO_2 nanoparticle produced poor performance then plain PES membrane. In another study, Ahmad et al.[17] prepared PSF membrane with SiO_2 and found that the modified membrane had bigger pore size with consistent surface pores. Permeation for the modified membrane was 16 times higher than plain membrane. Fouling of PSF membrane with humic acid was also studied and TiO_2 nanoparticles were used to modify the membrane.[18] They found that modified membranes had better resistance towards fouling specially those due to concentration polarization, cake layer formation and adsorption. ZnO nanoparticles were used as alternate to TiO_2.[19,20] It was used as hydrophilic modifier to polymeric membrane as well as pore forming agent. Various literatures associated to nanoparticle addition for modification of polymeric membranes are reported in Table 1.

From the table it may be envisaged that even though a number of authors have reported the addition of various nanoparticles to polymeric membrane, but the effect of polymeric nanoparticle as additives on polymeric membranes is scant and nobody studied the effect of chitosan-polyacrylic acid (CS-PAA) nanoparticle on polymeric membrane. In

addition, main problem with inorganic nanoparticles is their non-uniform dispersion due to agglomeration and high viscosity of the membrane casting solution. This results in pore blockage and lower flux.[16] Therefore, in this study cross-linked CS-PAA nanoparticles were synthesized and blended in PSF membrane casting solution in order to increase the hydrophilicity and fouling resistant behaviour of PSF membrane. As both component of CS-PAA nanoparticle contain large number of hydrophilic group of –OH, –COOH and $–NH_2$ in their structure. Also, CS-PAA nanoparticles are non-poisonous as they are generally used as carrier for drug delivery.[32] Additionally the strong hydrogen bonding between –S=O group of PSF and –OH group of nanoparticles,[33] make them compatible for blending and prevents the peeling off the nanoparticles from membrane (shown in Figure 1).

The present study focused on the synthesis and characterization of CS-PAA nanoparticle cross-linked with glutaraldehyde. Nanoparticle was characterized by Fourier transform infrared spectroscopy (FTIR) and photon correlation spectroscopy (PCS). PCS shows the size and zeta potential of nanoparticle and it also confirms the stability of CS-PAA nanoparticle in different pH condition. Morphology and composition of the fabricated membranes were analyzed by field emission scanning electron spectroscopy (FESEM) and attenuated total reflection–FTIR (ATR–FTIR). Prepared membranes were also characterized by atomic force microscopy (AFM). Further, fabricated membranes were analyzed by pure water flux (PWF), hydraulic permeability, BSA adsorption, hydrophilicity and UF performance during BSA separation. Finally, different fouling values i.e. total fouling, reversible and irreversible fouling caused during BSA ultrafiltration was calculated.

2. Experimental

2.1. Materials

PSF (average M_w = 35000 $gmol^{-1}$) and chitosan (medium molecular weight) were supplied from Sigma-Aldrich Co., USA. Synthesis grade acrylic acid (AA), PEG (average M_w = 4000 $gmol^{-1}$), Potassium persulphate ($K_2S_2O_8$) and Glutaraldehyde (GA) were procured from Merck, India. BSA of 68,000 $gmol^{-1}$ molecular weight was obtained from Otto Chemie Private Limited, India. FTIR grade potassium bromide (KBr) and reagent grade N-methylpyrrolidone (NMP) were purchased by LOBA Chemie, India. All the experiments were done by deionized (DI) water purified by Millipore system (Millipore, France).

2.2. Synthesis and characterization of CS-PAA nanoparticle

CS-PAA nanoparticles were synthesized by polymerization of acrylic acid (AA) in chitosan (CS) solution. In short; 1 g of CS was dissolved in 50 ml AA solution containing 1 g of AA. When the solution became clear, temperature of the mixture was raised to 80 ^oC and $K_2S_2O_8$ was added as initiator for polymerization under nitrogen atmosphere. The solution turns to milky in colour after 2 h of reaction. The temperature was lowered to 40 ^oC and a determined amount of GA (glucosamine unit in CS: aldehyde unit in GA = 1.1: 1) was added to the system as cross linker and reaction was carried out for further 2 h. Finally, the reaction mixture was centrifuged at 6000 RPM and obtained nanoparticles were kept aside for further characterization and modification of membrane.

The physicochemical properties of synthesized nanoparticles were studied by means of FTIR and photon correlation spectroscopy (PCS). FTIR (IRAffinity-1, Shimadzu, Japan) studies were performed for the verification and to look into the complex formation between chitosan and poly acrylic acid (PAA). The hydrodynamic size distribution and zeta potential of the CS-PAA nanoparticles was done by PCS (Delsanano, Bckman Coulter, Switzerland).

For the zeta potential analysis each sample was adjusted to a concentration of 0.1 % (w/w) in 10 mmol/L sodium chloride solution.

2.3. Fabrication of polymeric nanoparticle blended membranes

Centrifuged nanoparticles were dispersed in equal amount of water, so that it should appear as a solution. 10 g of dispersed nanoparticles were vigorously mixed with 100 ml of NMP at 60 ^{o}C. On the other hand, 30 wt % of PSF was dissolved in NMP with 2 wt % of PEG 4000 as pore forming agent. To this 30 wt % PSF solution, different amount of dispersed nanoparticle solution was mixed and required amount of NMP was added to get 15 wt % of PSF in final casting solution. This casting solution was briskly stirred at 60 ^{o}C for 12 h and after that degassed by ultra sonication for 30 minute. Finally the membranes were prepared by phase inversion process with a uniform thickness of 200 μm. Coagulation bath used for the phase inversion process contained DI water at room temperature (25 ^{o}C). After the immersion in the coagulation bath, the casted film immediately changed to white colour and separated out from the glass plate. Thereafter, the fabricated membrane was immersed in fresh DI water for overnight to remove any residual solvent. Steps for the modified membrane preparation is shown in Figure 2. Composition and viscosity of all the membrane casting solutions are provided in table 2. Viscosity of the membrane casting solutions was measured with a constant shear rate of 50 s^{-1}.

2.4. Membrane characterization

The presence of CS-PAA nanoparticle in the fabricated membrane was confirmed by ATR-FTIR. Comparison in the cross sectional and top surface morphology of the plain membrane and modified membranes was done by images obtained by FESEM (Make: Zeiss LSM 510 Meta). In addition, roughness of top surface of the prepared membranes were

measured and compared by AFM in the size of 5μm × 5μm size. It also provided the dispersion of the nanoparticle in blended membrane. Hydrophilicity of the membrane surface was précised by measuring water contact angle (CA) between water droplet and membrane surface. For all the prepared membranes, multiple CA values were measured and average was considered. Further, BSA adsorption experiment was also performed to evaluate the fouling resistance property of the membranes. Firstly, membrane samples were put in vials, containing 4 ml of phosphate buffer and kept in there for 1 h at 25 ^{o}C. After that, phosphate buffer solution was replaced with same amount of 1000 ppm BSA solution and incubated for 12 h at 25 ^{o}C. The amount of adsorbed BSA was measured by UV-VIS spectrophotometer at wavelength of 280 nm. Multiple replicate experiments were done for every membrane samples. The porosity (ε) of the membranes was determined by gravimetric method, using following equations:[34]

$$\varepsilon = \frac{W_1 - W_2}{A \times l \times d_w} \quad (1)$$

Here, W_1, W_2, A, l and d_w are the weight of wet membrane, weight of dry membrane, area of membrane, thickness of membrane and density of water (0.998 g/cm^3), respectively. A digimatic measuring unit (model: Litematic, VL 50, Mitutoyo, Japan) was used for the measurement of membrane thickness at 10 different places and average value was considered.

Mean pore radius of the membrane was calculated by Guerout–Elford–Ferry equation (equation (2)).[35] This equation is based on porosity and pure water flux data.

$$r_m = \sqrt{\frac{(2.9 - 1.7\varepsilon) \times 8\eta l Q}{\varepsilon \times A \times \Delta P}} \quad (2)$$

Here, η is the viscosity of water at 25˚C, Q is the volume of water permeated per unit time (m^3/s), and ΔP is the operating pressure.

2.5. Pure water permeation and BSA ultrafiltration experiments

Fabricated membranes were first compacted with DI water at transmembrane pressure of 400 kPa for 2 h and flux was measured for regular time intervals. Thereafter, water permeation at different transmembrane pressure (upto 400 kPa) through the compacted membranes was measured and hydraulic permeability (L_m) was calculated using this information. The flux was calculated by the following equation:

$$J_w = \frac{V}{A\Delta t} \tag{3}$$

Here, J_w, A, V and Δt denote pure water flux (L/m^2 h), effective membrane area (m^2), volume of water permeated (L) and permeation time (h), respectively. Hydraulic permeability (L_m) (L/m^{2}h kPa) was calculated as:

$$P_m = \frac{J_w}{\Delta P} \tag{4}$$

For estimation of fouling during BSA ultrafiltration process, initially all the membranes were compacted at 400 kPa for 30 minute. Subsequently, pressure was reduced to 300 kPa. After the 90 minute of water permeation, steady state water flux was measured and termed as J_{w1}. Afterwards, feed solution was switched to 1000 ppm BSA solution. BSA flux at the end of next 90 minute was called as J_{BSA}. BSA rejection was measured UV-VIS spectroscopy by using following formulae:

$$R(\%) = \left(1 - \frac{C_{BSA}^{permeate}}{C_{BSA}^{feed}}\right) \times 100 \tag{5}$$

Here, $C_{BSA}^{permeate}$ and C_{BSA}^{feed} represents BSA concentration in permeate and feed respectively. After BSA ultrafiltration, membranes were washed with pure water flushing. Finally, again pure water was permeated through membranes and steady state PWF was measured at the end of 90 minutes and labelled as J_{w2}.

3. Results and discussion

3.1. FTIR and PCS analysis

For the confirmation and to investigate the complex formation between PAA and chitosan, FTIR study was performed. Figure 3 shows the FTIR of CS, AA and CS-PAA nanoparticles. The main peaks can be assigned as follows: 3421cm^{-1} (O–H stretching vibration), 2951 cm^{-1} and 2897 cm^{-1} (C–H stretching related to glutaraldehyde, 1736 cm^{-1} (peak of the carboxyl group of PAA), 1624 cm^{-1} (peak of NH_2 of CS), 1521 cm^{-1} and 1400 cm^{-1} (symmetric and asymmetric stretching vibrations of COO^- anion groups), 1284 cm^{-1} and 1076 cm^{-1} (C–O group). The peaks of COO^- anion groups (1521 cm^{-1} and 1400 cm^{-1}) are not present in FTIR analysis of AA, as they appears due to the complex formation between in CS and PAA. Also intensity of peak at 1736 cm^{-1} is much lower in CS-PAA compared to AA, due to complex formation.

The particle size distribution and zeta potential of the CS-PAA nanoparticles in different pH conditions were characterized by PCS (Figures 4 and 5). The hydrodynamic size of CS-PAA nanoparticle is found to change with change in pH. The size of nanoparticle attains the minimum value at pH 4, and becomes considerably bigger in size at pH 1 and much bigger at pH 7.5. At low pH of 1, the CS is fully ionized and form $-NH_3^+$. Thus, the CS-PAA nanoparticles become larger due to electrostatic repulsion between $-NH_3^+$ groups and increase in size is observed. At pH 7.5, the situation is opposite; here PAA is fully ionized and form -COO^- groups. Thus, the electrostatic repulsion between -COO^- groups of

PAA causes the increase in the size of CS-PAA nanoparticle. Also, this study confirms the stability of nanoparticle in different pH conditions due to the cross linking with GA.[32] On the other hand, zeta potential shows a monotonous trend and keeps decreasing with the increase in pH. Though, when the pH reaches 7.5, a negative zeta potential is observed. The adsorption of anions such as OH^- is the reason of negative zeta potential at pH above 7.[36] These changes in hydrodynamic size and zeta potential with pH are attributed to the presence of amine and carboxyl group in nanoparticle and could be helpful for antifouling property of membranes.

ATR-FTIR spectra of plain and modified PSF membranes surfaces fabricated with different wt % of CS-PAA nanoparticles are shown in Figure 6. Peak appears around 1626 cm^{-1}, confirms the presence of NH_2 group present in chitosan. Another new peak appears at around 1741 cm^{-1}, which confirms the presence of –COOH group, polyacrylic acid segment of CS-PAA nanoparticle. The intensity of both these peaks is highest for membrane M30, as it contained highest quantity of CS-PAA nanoparticle. The peaks at 1155 cm^{-1} and 1295 cm^{-1} are due to –C–O–C– and S=O group present in polysulfone.

3.2. Hydrophilicity and BSA adsorption study of the membranes

Water contact angle of the top surface of membranes reveal the hydrophilicity of the membrane. It explains the wettability of the membrane, as it could enhance the fouling resistance as well as flux through membranes.[13,23] The initial water contact angle measured on the top surface of membrane, just after the DI water dropped on it; reflects the natural wettability of the membrane. As represented in Figure 7, water contact angle decreased considerably with the addition of CS-PAA nanoparticle. Plain membrane had the highest contact angle of 72 ± 1.5^{o}. With the increase in quantity of CS-PAA nanoparticle in membrane

matrix, contact angle reduced from 68±1.5^{o} to 54±1^{o} for membranes M10 and M30, respectively. The reduction in contact angle leads to the enhancement of hydrophilicity of the membrane, which induces from the $–NH_2$ and –COOH group present in the nanoparticle. This is the reason, as the quantity of CS-PAA nanoparticle increases, the contact angle decreases i.e. hydrophilicity of membrane enhances.

It has been conversed that with the increase in quantity of CS-PAA nanoparticle, surface hydrophilicity of the modified membranes had increased. Figure 7 shows the amount of adsorbed BSA on the unit surface area of membranes. It can be seen that modified membranes showed more resistance against the adsorption of BSA. In fact, plain membrane M00 adsorbed almost 4 times higher amount of BSA then modified membrane M30. Reason behind low amount of BSA adsorption is the presence of $–COO^-$ group in CS-PAA nanoparticle. As we know that the isoelectric point of BSA is about pH 4.7; it means that above this pH it remains negatively charged and below this pH it remains positively charged. On the other hand PAA has deprotonation pH of around 4.8, so above pH 5, membrane and BSA both have negative charge. Thus, membrane surface electrostatically repels the BSA molecule.

3.3. Microscopic study of membranes

Figure 8 shows the AFM images of top surface of plain and modified membrane with roughness parameters. AFM images illustrated that top surfaces of membrane have nodule aggregates, this results in rough membrane surface. It can be observed that, as the nanoparticle quantity has been increased the nodule size on membrane surface is getting smaller. Further, due to smaller nodule size, the overall roughness of the modified membranes is lesser compared to plain membrane. RMS roughness values are 11.35, 8.08,

5.10 and 3.95 for membranes M00, M10, M20 and M30 respectively. It was stated that membrane with comparatively smoother surfaces has better resistance to fouling.[37] Therefore, the modified membranes show the possibility of fouling resistance behaviour. Hence, these results are in line with BSA adsorption results.

Figure 9a shows the top surface FESEM images of the plain and blended PSF membranes. As can be seen, the amount of CS-PAA nanoparticle on membrane surface has been enlarged by increasing the quantity of nanoparticle in membrane casting solution. From the FESEM images, it can be see that despite the increasing quantity of nanoparticle in membrane casting solution, their dispersion in membrane is uniform. The dispersion of nanoparticle in membrane top surface is in agreement with the hydrophilicity result of membranes, as it was stated that well dispersed nanoparticles enhances the hydrophilicity with increase in quantity compared to agglomerated nanoparticles.[16, 38] Compared to previous studies with inorganic nanoparticles, the polymeric nanoparticles are more dispersed. The possible reason is polymer-polymer interaction is stronger compared to polymer-non-polymer interaction. Also flux data shows that polymeric nanoparticles are well dispersed, as there was increment in flux with increase in nanoparticle quantity.

Figure 9b shows the cross section image of all the prepared membranes. All the membranes have asymmetric structure, it consist top dense skin layer. Below the skin layer membranes have porous sub layer containing finger like structure. At high magnification one can see the dispersed nanoparticle in modified membranes. But with higher quantity of nanoparticle (membrane M20 and M30), it can be observed that finger like macrovoids became longer and prominent compared to plain membrane. In case of membrane M10, there is no significant change in cross sectional morphology can be observed, it is all most like membrane M00. This can be correlated to kinetic and thermodynamic effects. The ratio of nonsolvent (water) inflow and solvent (NMP) out flow during the phase change process

increases with increase in the hydrophilicity of the membrane casting solution induced with hydrophilic nanoparticle.[23, 39] Also, this change in cross sectional morphology may be attributing to the increase in viscosity of membrane casting solution with the addition of nanoparticle. At higher magnification, one can clearly spot the dispersed nanoparticle in cross section of modified membrane.

Table 3 shows the overall porosity and average pore size of prepared membranes. Porosity of all the membranes is almost same but average pore size is increased with the incorporation of more quantity of nanoparticles in modified membranes. As it is described earlier that the addition of CS-PAA nanoparticle increases the thermodynamic instability of casting solution in the coagulation bath, it supports the rapid demixing.[40] This results in large pore formation with the increase in amount of nanoparticle.

3.4. Pure water flux and hydraulic permeability

Figure 10a shows constant pressure (400 kPa) flux during compaction; it was used to calculate the compaction factor (CF) for prepared membrane (shown in Table 3). CF describes the membrane sub layer structure. Existence of big macro voids in membrane sub layer is the reason of compaction. Initially flux declines sharply for all the membranes but after 30 minutes it remains nearly steady. During compaction pore walls become closer, denser and uniform, that results in reduction in size of pores in addition to the flux.[41] The steady state PWF increases with increase in quantity of nanoparticle. Steady state flux for plain membrane M00 and membrane M30 was 54 L/m^2h and 112.8 L/m^2h, respectively. Permeation flux through the membranes depends upon surface pore size, skin layer thickness, cross sectional morphology of membrane, viscosity of membrane casting solution and hydrophilicity of membrane. It is shown in Figure 7 that addition of CS-PAA nanoparticle

led to decrease in water contact angle and enhancement in the hydrophilicity of the prepared membranes. The increase in steady state flux is due to increase in hydrophilicity as well as increase in average pore size. Table 3 shows the hydraulic permeability (P_m) of the membranes, calculated with the help of Figure 10b. P_m was increased significantly from 0.146 to 0.265 L/m^2 h kPa (Table 3) for plain membrane to modified membrane with maximum quantity of nanoparticle. Findings of the pure water permeability and hydraulic permeability studies evidently show that addition of CS-PAA nanoparticles improves the pore size and hydrophilicity, which affect the permeability. These results of PWF and hydraulic permeability are in line with the results of previous studies using metal oxide nanoparticle.[21, 22, 42]

3.5. Fouling resistant characteristic of membranes by BSA ultrafiltration experiment

The antifouling property of prepared membranes was studied by dynamic fouling resistance experiment. This process was recorded and shown in Figure 11. DI water flux was measured from 0 - 90 min and 180 - 270 min, while BSA flux was measured from 90 - 180 min. Flux measured at the end of 90, 180 and 270 minute were called as J_{w1}, J_{BSA} and J_{w2} respectively. It was observed that during BSA permeation, a sudden flux loss was seen in initial permeation for all the membranes. Earlier flux loss during BSA ultrafiltration is caused by adsorption or deposition of BSA molecules inside the pores or on the membrane surface. It is significant to note that blended membranes have higher BSA flux then plain membrane. It was stated that the more hydrophilic the membrane was, the less extent of fouling.[43] Also, it was discussed earlier that modified membranes adsorbed less quantity of BSA compared to plain membrane. So, the fouling resistance membrane should efficiently resist the adsorption or deposition of foulants to their surface or pore as reported in literatures.[44, 45] Total fouling

(F_t) can be categorised as reversible and irreversible fouling. Adsorption or deposition of foulants, which can be cleaned by normal hydraulic flushing, is named as reversible fouling (F_r). On the contrary irreversible adsorption of membrane can only be removed by chemical cleaning and it is termed as irreversible fouling (F_{ir}). These values were estimated by following equations:

$$F_t = 1 - \left(J_{BSA}/J_{w1}\right) \tag{6}$$

$$F_r = (J_{w2} - J_{BSA})/J_{w1} \tag{7}$$

$$F_{ir} = (J_{w1} - J_{BSA})/J_{w1} \tag{8}$$

With the help of J_{w1} and J_{w2}, flux recovery ratio ($Flux_{RR}$) was measured using the following equation:

$$Flux_{RR}(\%) = \frac{J_{w2}}{J_{w1}} \times 100 \tag{9}$$

Figure 12 shows the different fouling values and flux recovery ratio for fabricated membranes. The unmodified membranes has the much lower value of total fouling and irreversible fouling compared to the plain PSF membranes and as a result, higher value of flux recovery ratio. Addition of CS-PAA nanoparticle resisted the deposition or adsorption of BSA molecule on membrane surface or inside the membrane pores by enhancing the hydrophilicity and also by electro static repulsion. Due to this reason, as the quantity of CS-PAA nanoparticle was amplified in the membrane, irreversible fouling was reduced in modified membranes. Moreover, reduction in irreversible fouling enhances the flux recovery ratio for modified membranes. As flux recovery ratio is directly associated to irreversible fouling. The flux recovery ratio for plain membrane was merely just about 41.5 %, whereas it was reached to 88.6 % for membrane M30. The superior fouling resistance behaviour of the

CS-PAA blended membrane probably attributed to the bulk presence of carboxyl, amine and hydroxyl groups on the surface of modified membranes resulted from setting of CS-PAA nanoparticles on the top surface of modified membranes (as shown in Figure 9a). This causes the reduction in water contact angle and BSA adsorption (Figure 7). The more hydrophilic surface can easily form a pure water layer and repel the deposition of hydrophobic foulants.

As shown in Figure 13, BSA flux through prepared membranes was increased with the increase in CS-PAA nanoparticle quantity in membrane. BSA flux for membrane M30 was measured around 24.3 L/m^2h compared to 8.2 L/m^2h for plain membrane. It is almost 3 time higher flux for membrane M30 with respect to plain membrane. It was discussed earlier that CS-PAA nanoparticle enhances the hydrophilicity as well as it also enhances the pore size and its formation. Also, may be due to higher flux and increase in pore size caused a little drop in BSA rejection with the increasing quantity of nanoparticle. BSA flux reduced from 90.5 % for plain membrane to 86.4 % for modified membrane M30.

4. Conclusion

Cross linked CS-PAA nanoparticles were synthesized by polymerization of AA in CS solution and characterized by FTIR and photon correlation spectroscopy. These nanoparticles were blended in different quantity for the modification PSF membrane. All the membranes fabricated in this study, were characterized by, FESEM, AFM, ATR-FTIR, BSA adsorption, water contact angle, mean pore size, PWF and BSA UF for fouling behaviour. The results are condensed as follows: (a) Prepared CS-PAA nano particles shows change in hydrodynamic size with change in pH due to the presence of amine and carboxyl group. (b) Top surface FESEM images of modified membranes confirmed the consistent dispersion of CS-PAA nanoparticle. (c) Cross sectional images demonstrated that all the membranes had asymmetric

structure, but in modified membranes finger like macro-voids became longer and prominent. (d) Blending of CS-PAA nanoparticle increased the hydrophilicity, surface smoothness and pure water flux through membranes. It also affected the mean pore size of blended membranes. (e) Addition of CS-PAA nanoparticle caused decrease in BSA adsorption, which in result decreased the irreversible fouling of the modified membranes.

Acknowledgement

This work is partially supported by a grant from the Indian National Science Academy (INSA), New Delhi. Any opinions, findings and conclusions expressed in this paper are those of the authors and do not necessarily reflect the views of INSA, New Delhi.

Nomenclature

A	effective membrane area (m^2)
ATR	attenuated total reflectance
BSA	bovine serum albumin
$C_{BSA}^{permeate}$	BSA concentration in permeate
C_{BSA}^{feed}	BSA concentration in feed
CF	compaction factor
CS	Chitosan
d_w	density of water
ε	porosity
F_{ir}	irreversible fouling
F_r	reversible fouling
F_t	total fouling
FESEM	field emission scanning electron microscope
FTIR	Fourier transform infrared spectroscopy
GA	Glutaraldehyde
h	hour
η	viscosity
J_w	BSA flux
J_w	pure water flux (L/m^2 h)
J_{w1}	initial water flux (L/m^2 h)
J_{w2}	water flux in second run (L/m^2 h)
L	thickness of membrane
NMP	N-methyl-2-pyrrolidone
NMR	nuclear magnetic resonance
NOM	natural organic matter
ΔP	pressure (kPa)
PAA	Polyacrylic acid
PCS	photon correlation spectroscopy
PEG	polyethylene glycol

PES	polyethersulfone
P_m	hydraulic permeability (L/m^{2}h kPa)
PSF	polysulfone
PWF	pure water flux
Q	volume of water permeated (L)
r_m	mean pore radius
Δt	permeation time
TMP	transmembrane pressure
UF	ultrafiltration
WCA	water contact angle
W_d	weight of dry membrane
W_w	weight of wet membrane

References

1 S.S. Madaeni, *Water Res.*, 1999, **33**, 301-308.

2 R. Ghosh and Z.F. Cui, *J. Membr. Sci.*, 2000, 167, 47-53.

3 D.Wu and M.R. Bird, *J. Food Proc. Eng.*, 2007, **30**, 293-323.

4 Y. Zhang, Z. Jin, X. Shan, J. Sunarso and P. Cui, *J. Hazard. Mater.*, 2011, **186**, 390-395.

5 J.C. Schrotter and B. Bozkaya-Schrotter, *Membrane Technology*, Wiley-VCH, New York, 2010.

6 I.N.H.M. Amin, A.W. Mohammad, M. Markom, C.P. Leo and N. Hilal, *J. Membr. Sci.*, 2010, **351**, 75-86.

7 Y.H. Cho, J. Han, S. Han, M.D. Guiver and H.B. Park, *J. Membr. Sci.*, 2013, **445**, 220-227.

8 D.L. Arockiasamy, A. Nagendran, K.H. Shobana and D. Mohan, *Sep. Sci. Technol.*, 2009, **44**, 398-421.

9 R. Malaisamy, R. Mahendran, D. Mohan, M. Rajendran and V. Mohan, *J. Appl. Polym. Sci.*, 2002, **86**, 1749-1761.

10 S. Belfer, J. Gilron, Y. Purinson, R. Fainshtain, N. Daltrophe, M. Priel, B. Tenzer and A. Toma, *Desalination*, 2001, **139**, 169-176.

11 N. Nady, M.C.R. Franssen, H. Zuilhof, M.S.M. Eldin, R. Boom, and K. Schroën, *Desalination*, 2011, **275**, 1-9.

12 A. Idris, N.M. Zain and M.Y. Noordin, *Desalination*, 2007, **207**, 324-339.

13 M.K. Sinha and M.K. Purkait, *J. Membr. Sci.*, 2013, **437**, 7-16.

14 H.A. Tsai, L.D. Li, K.R. Lee, Y.C. Wang, C.L. Li, J. Huang and J.Y. Lai, *J. Membr. Sci.*, 2000, **176**, 97-103.

15 M.K. Sinha and M.K. Purkait, *J. Membr. Sci.*, 2014, **464**, 20-32.

16 A. Razmjou, J. Mansouri and V. Chen, *J. Membr. Sci.*, 2011, **378**, 73-84.

17 N. A. A. Hamid, A. F. Ismail, T. Matsuura, A. W. Zularisam, W.J. Lau, E. Yuliwati and M. S. Abdullah, *Desalination*, 2011, **273**, 85-92.

18 J. H. Li, Y. Y. Xu, L. P. Zhu, J. H. Wang and C. H. Du, *J. Membr. Sci.*, 2009, **326**, 659-666.

19 C.P. Leo, W.P.C. Lee, A.L. Ahmad and A.W. Mohammad, *Sep. Purif. Technol.*, 2012, **89**, 51-56.

20 V. Vatanpour, S. Siavash, L. Rajabi, S. Zinadini and A. Ashraf, *J. Membr. Sci.*, 2012, **401-402**, 132-143.

21 A. L. Ahmad, M. A. Majid and B.S. Ooi, *Desalination*, 2011, **268**, 266-269.

22 S. Balta, A. Sotto, P. Luis, L. Benea, B. Van Der Bruggen and J. Kim, *J. Membr. Sci.*, 2012, **389**, 155-161.

23 V. Vatanpour, M. Esmaeili and M.H.D.A. Farahani, *J. Membr. Sci.*, 2014, **466**, 70-81.

24 H.J. Song, Y.J. Jo, S.Y. Kim, J. Lee and C.K. Kim, *J. Membr. Sci.*, 2014, **466**, 173-182.

25 A.K. Nair, A.M. Isloor, R. Kumar and A. F. Ismail, *Desalination*, 2013, **322**, 69-75.

26 D.Y. Koseoglu-Imer, B. Kose, M. Altinbas and I. Koyuncu, *J. Membr. Sci.*, 2013, **428**, 620-628.

27 A. Mollahosseini, A. Rahimpour, M. Jahamshahi, M. Peyravi and M. Khavarpour, *Desalination*, 2012, **306**, 41-50.

28 J. Garcia-Ivars, M.I. Alcaina-Miranda, M.I. Iborra-Clar, J.A. Mendoza-Roca and L. Pastor-Alcañiz, *Sep. Purif. Technol.*, 2014, **128**, 45-57.

29 J. Yin, G. Zhu and B. Deng, *J. Membr. Sci.*, 2013, **437**, 237-248.

30 S. Zinadini, A. A. Zinatizadeh, M. Rahimi, V. Vatanpour, H. Zangeneh and M. Beygzadeh, *Desalination*, 2014, **349**, 145-154.

31 C. Dong, G. He, H. Li, R. Zhao, Y. Han and Y. Deng, *J. Membr. Sci.*, 2012, **387-388**, 40-47.

32 Y. Hu, Y. Chen, Q. Chen, L. Zhang, X. Jiang and C. Yang, *Polymer*, 2005, **46**, 12703-12710.

33 J. Emsley, *Chem. Soc. Rev.*, 1980, **9**, 91-124.

34 J. F. Li, Z. L. Xu, H. Yang, L. Y. Yu and M. Liu, *Appl. Surf. Sci.*, 2009, **255**, 4725-4732.

35 N.A.A. Hamid, A.F. Ismail, T. Matsuura, A.W. Zularisam, W.J. Lau, E. Yuliwati and M.S. Abdullah, *Desalination*, 2011, **273**, 85-92.

36 F. Liu and A. Eisenberg, *J. Am. Chem. Soc.*, 2003, **125**, 15059-15064.

37 X. Li, X. Fang, R. Pang, J. Li, X. Sun and J. Shen, *J. Membr. Sci.*, 2014, **467**, 226-235.

38 A. Rahimpour, S.S. Madaeni, A.H. Taheri and Y. Mansourpanah, *J. Membr. Sci.*, 2008, **313**, 158-169.

39 S. Majeed, D. Fierro, K. Buhr, J. Wind, B. Du, A. Boschetti-de-Fierro and V. Abetz, *J. Membr. Sci.*, 2012, **403-404**, 101-109.

40 F. Liu, M. R. M. Abed and K. Li, *J. Membr. Sci.*, 2011, **366**, 97-103.

41 M. Mulder, *Basic Principles of Membrane Technology*, Kluwer Academic Publishers, Dordrecht, 1991.

42 N. Maximous, G. Nakhla, W. Wan and K. Wong, *J. Membr. Sci.*, 2009, **341**, 67-75.

43 X. L. Li, L. P. Zhu, B. K. Zhu and Y. Y. Xu, *Sep. Purif. Technol.*, 2011, **83**, 66-73.

44 J.H. Huisman, P. Pradanos and A. Hermandez, *J. Membr. Sci.*, 2000, **179**, 79-90.

45 Q. Li, Q. Bi, H. Lin, L. Bian and X.Wang, *J. Membr. Sci.*, 2013, **427**, 155-167.

List of Tables

List of Figures

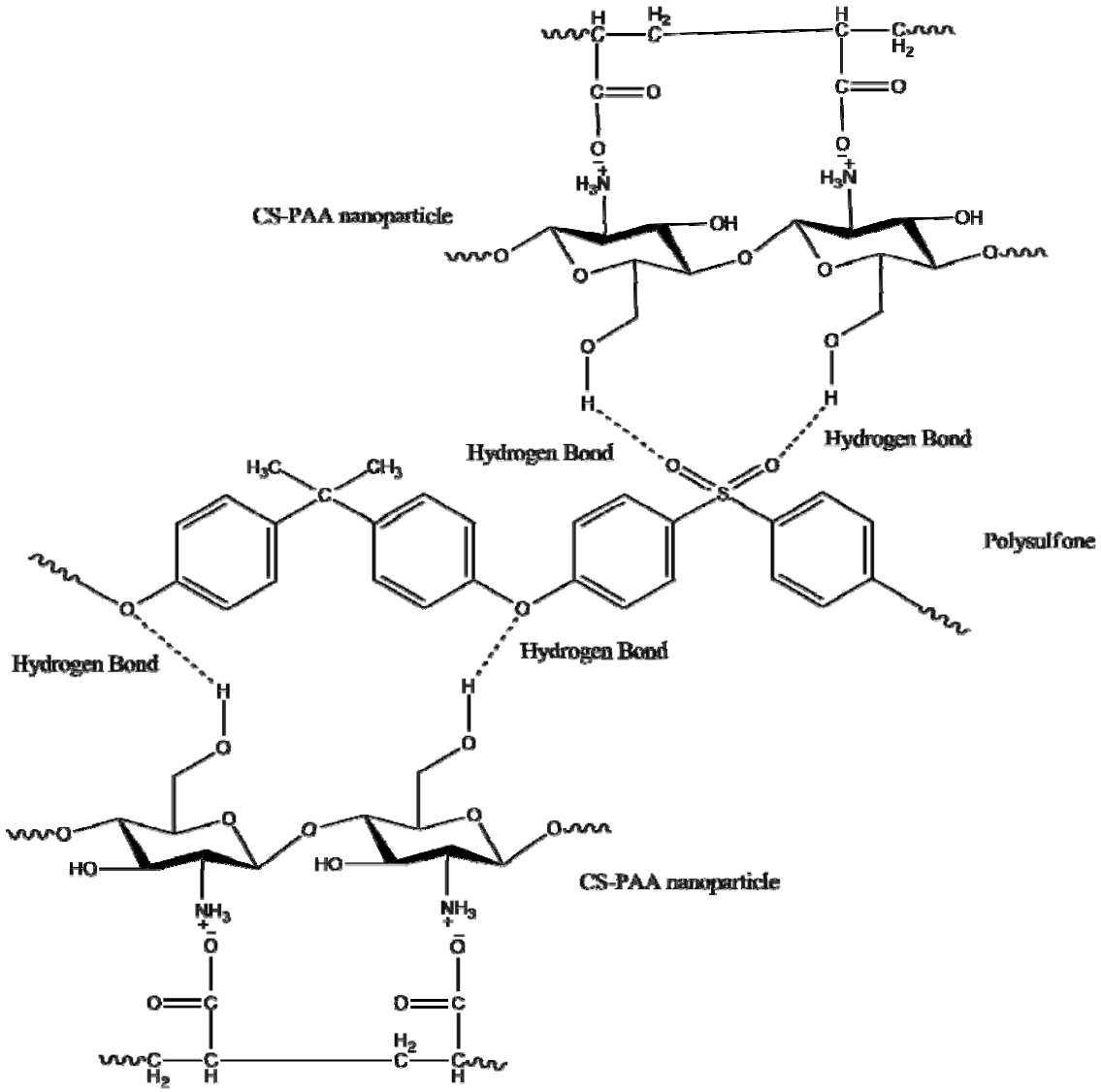

Figure 1: Possible H-bonding between –S=O group of PSF and –OH group of CS-PAA nanoparticles.

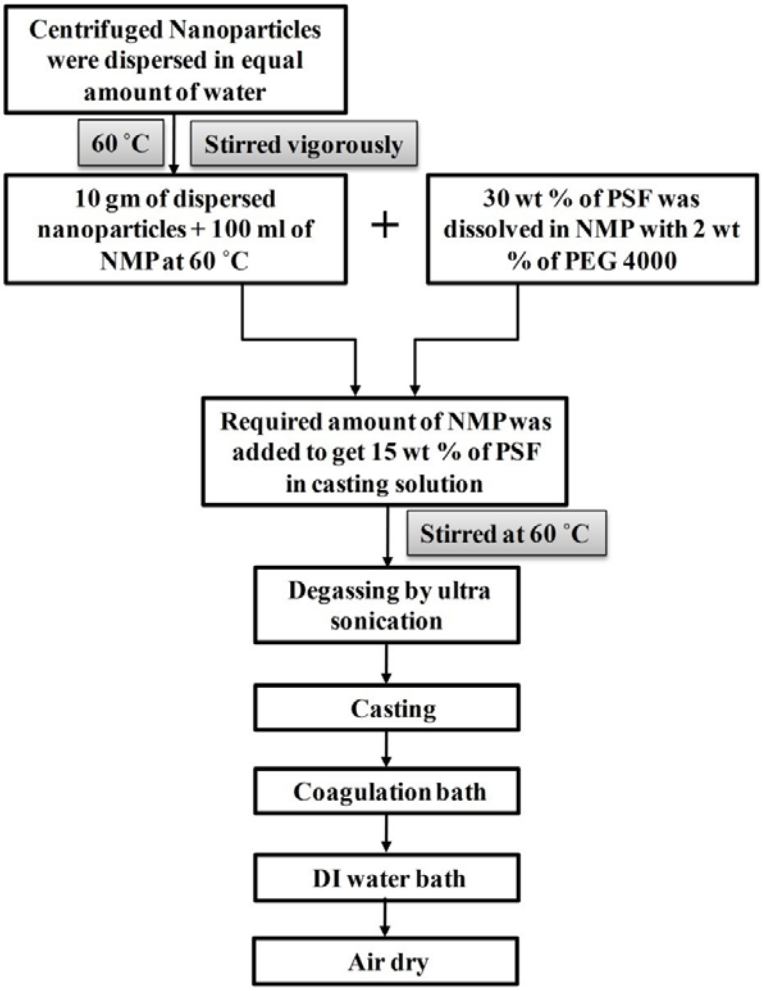

Figure 2: Steps for fabrication of modified membranes.

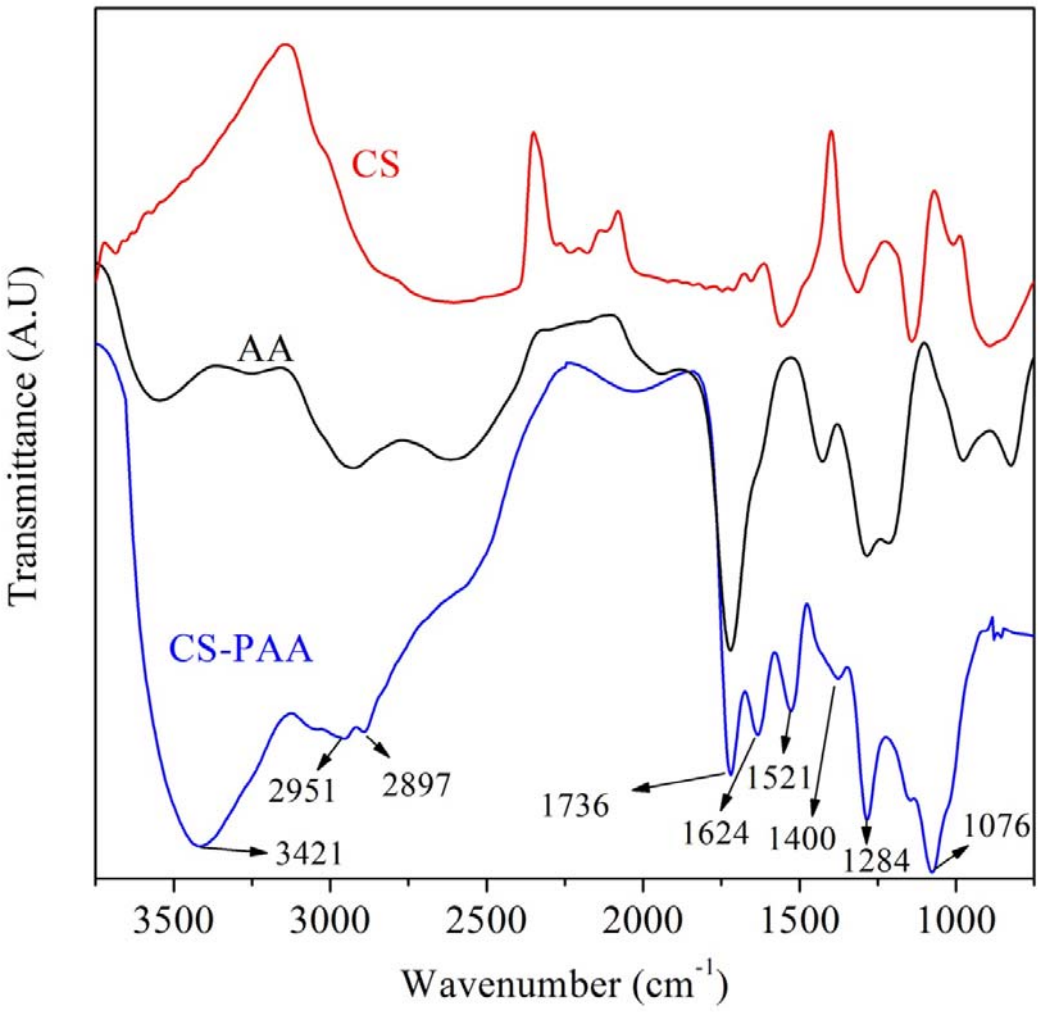

Figure 3: FTIR spectra of AA, CS and CS-PAA nanoparticle.

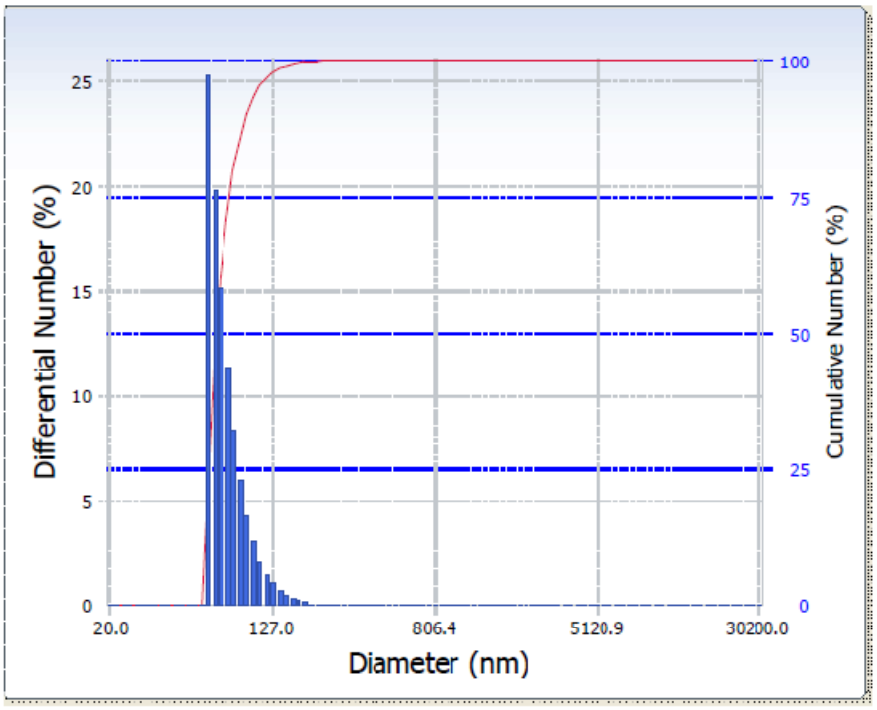

(a)

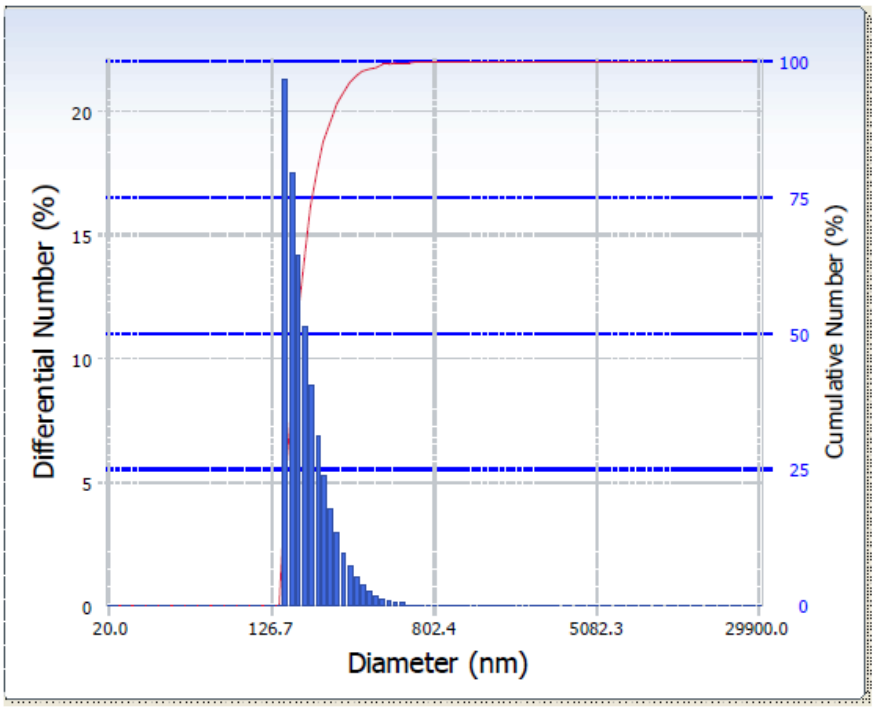

(b)

Figure 4: Size distribution of synthesized nanoparticle (a) at pH 4 (b) at pH 7.5.

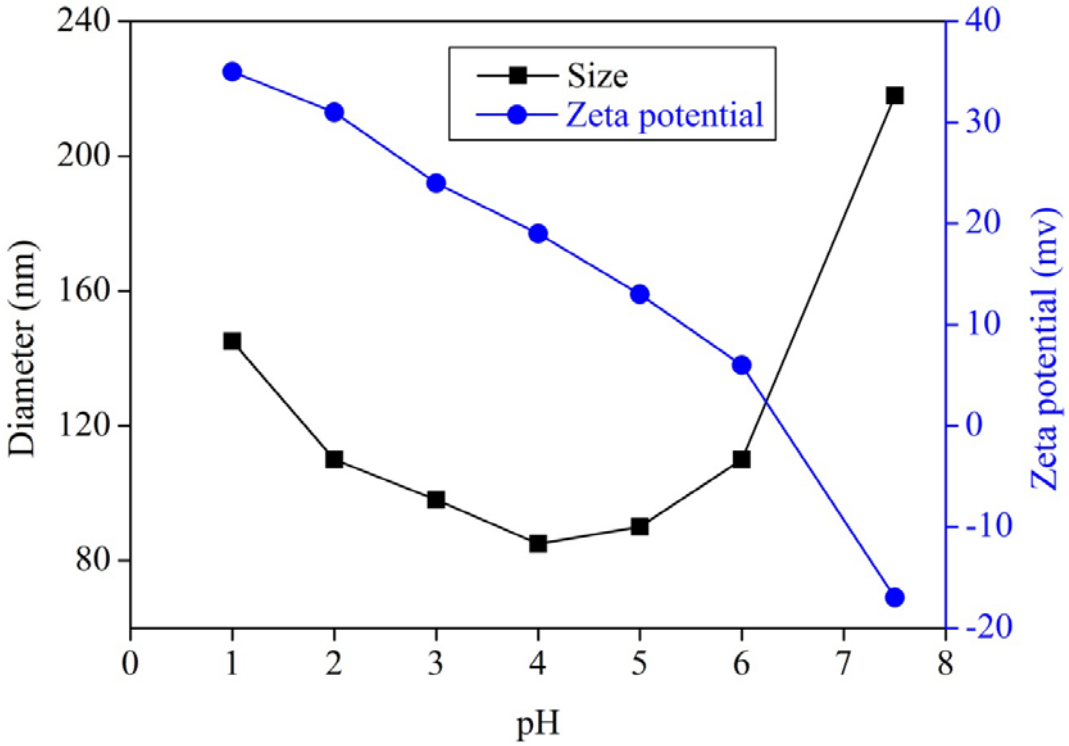

Figure 5: Effect of pH on CS-PAA nanoparticle size and zeta potential.

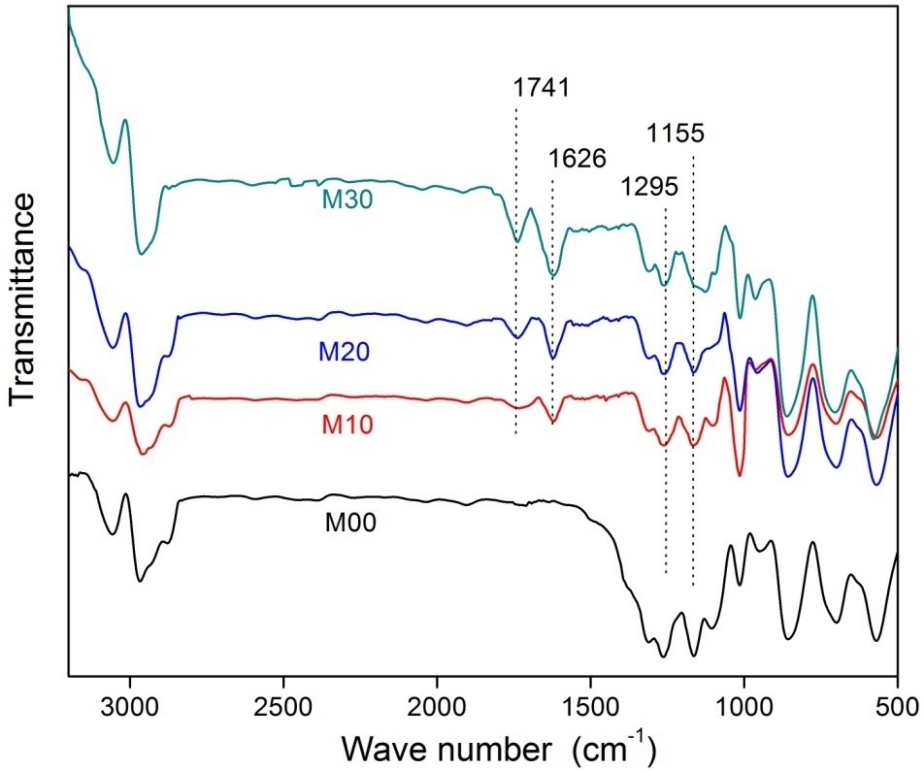

Figure 6: ATR-FTIR spectra of different membranes.

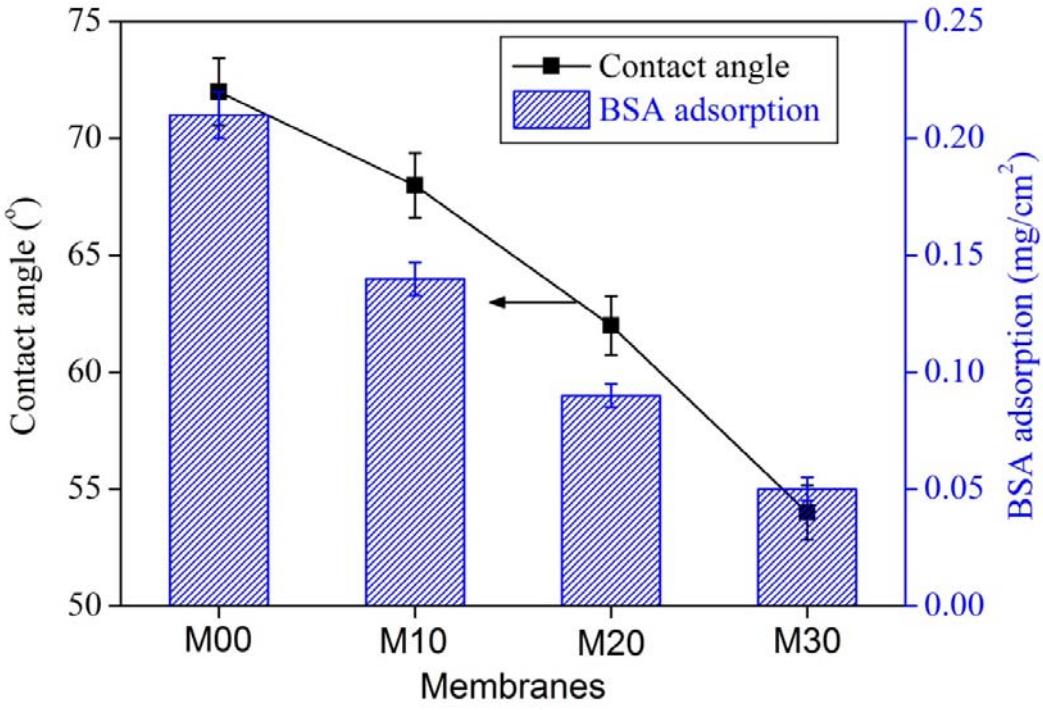

Figure 7: Hydrophilicity and BSA adsorption o values of prepared membranes.

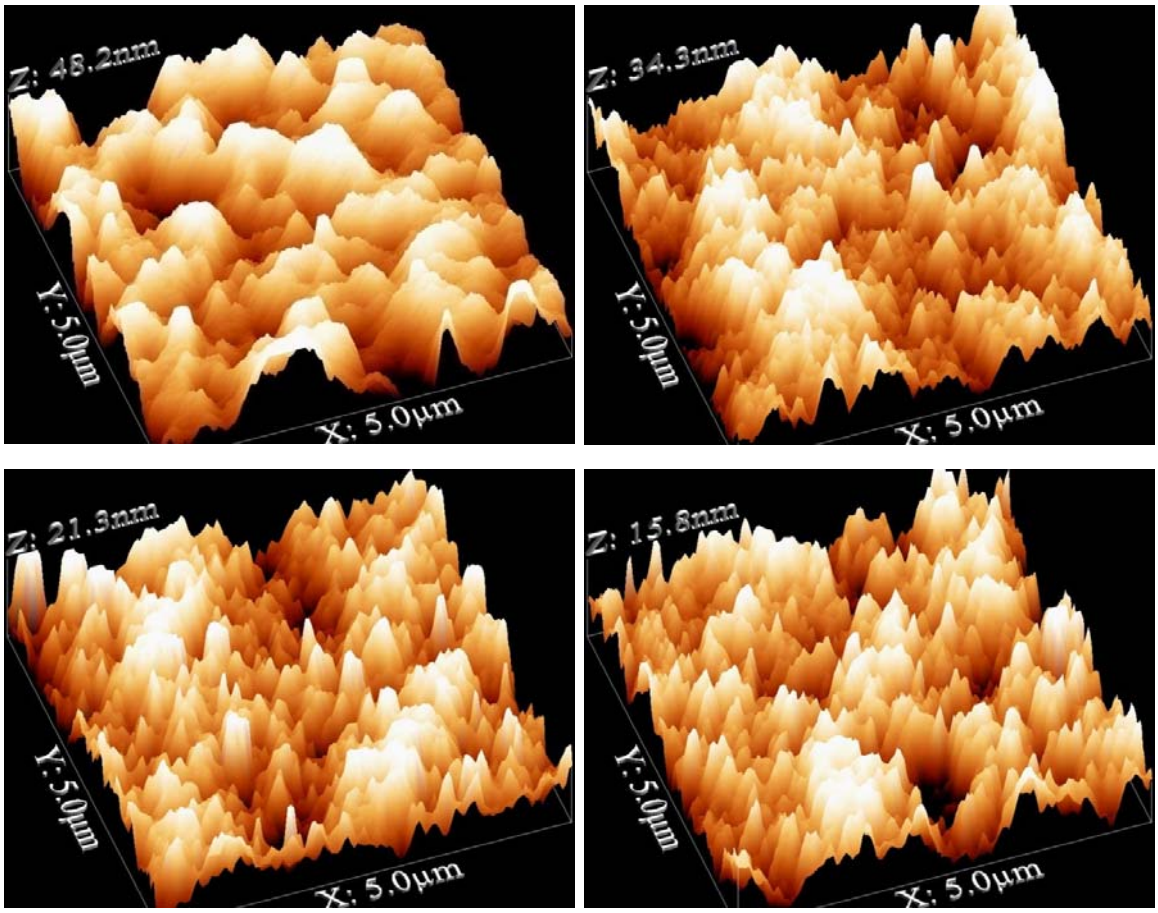

Figure 8: Three dimensional AFM images and roughness parameters of prepared membranes.

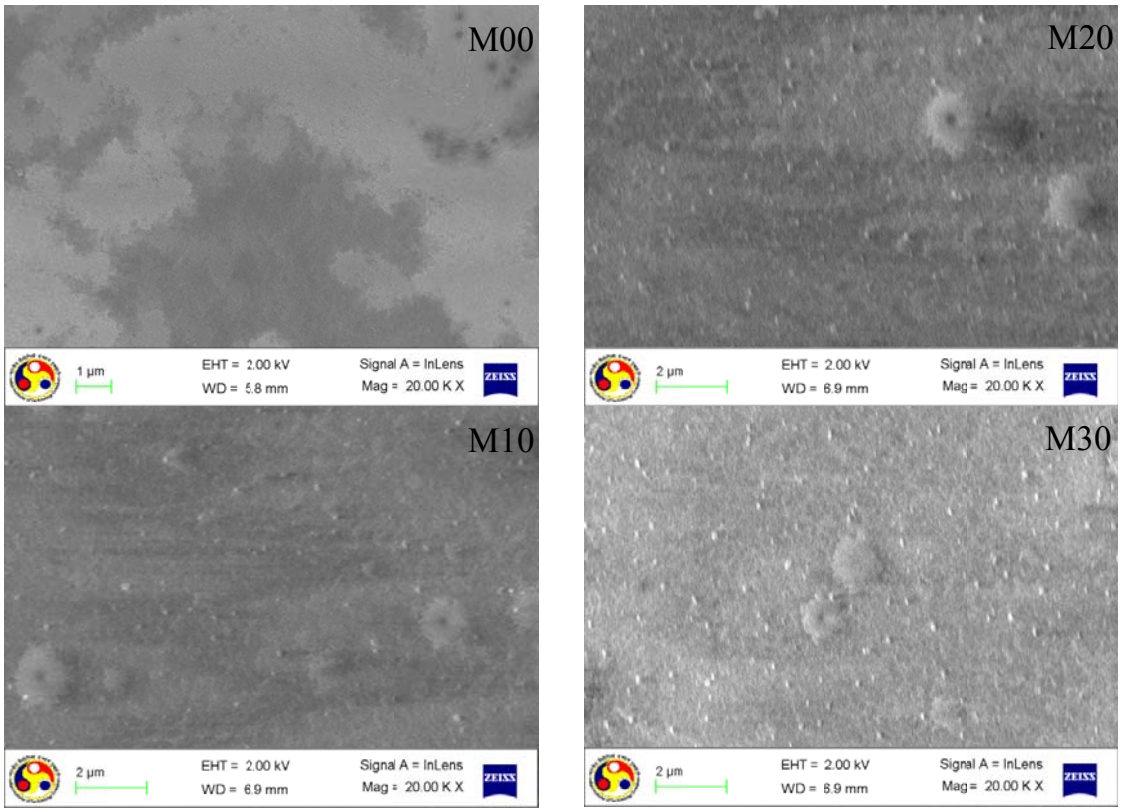

Figure 9a: Top surface FESEM images of prepared membranes.

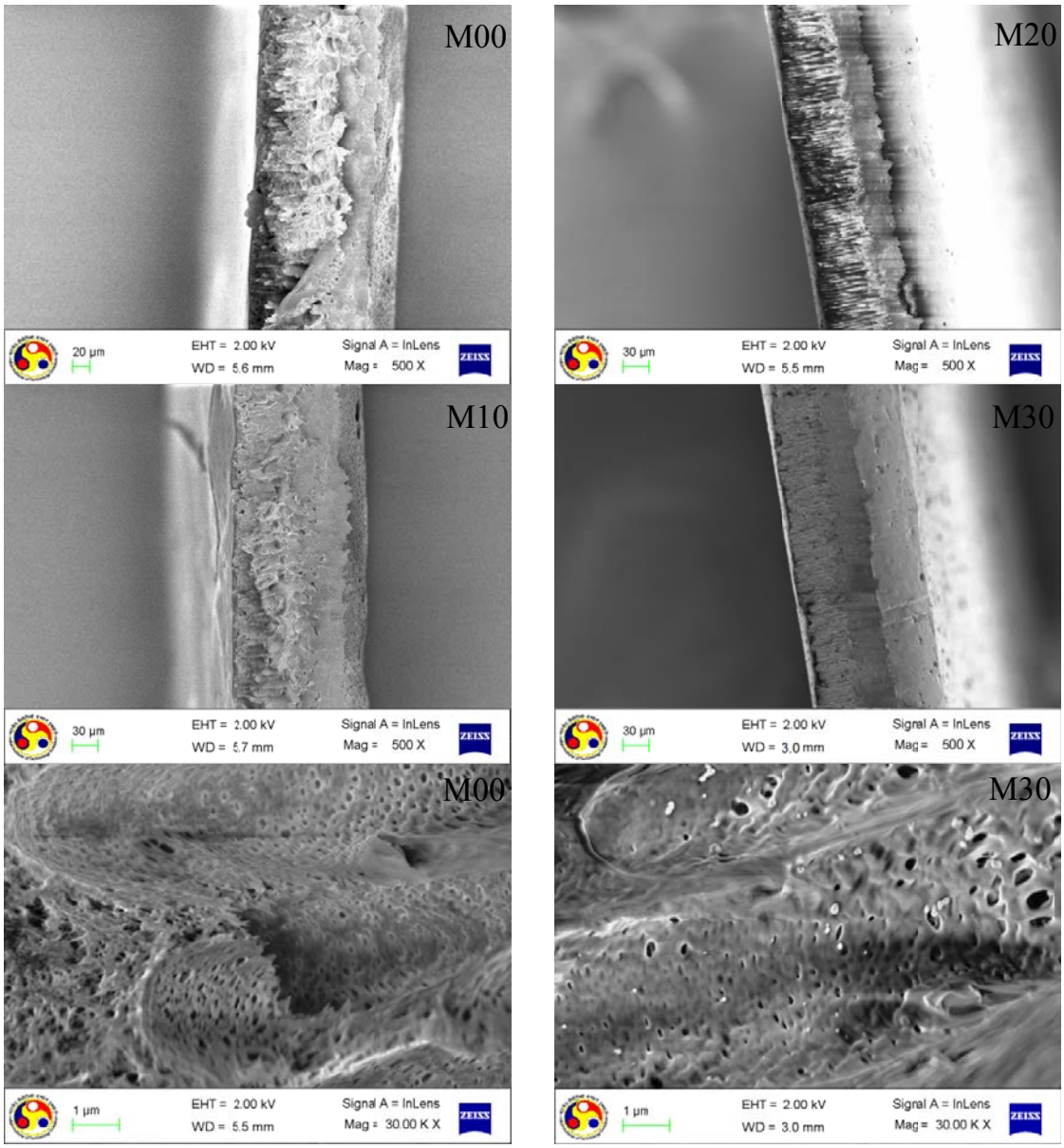

Figure 9b: Cross section FESEM images of plain and modified membranes.

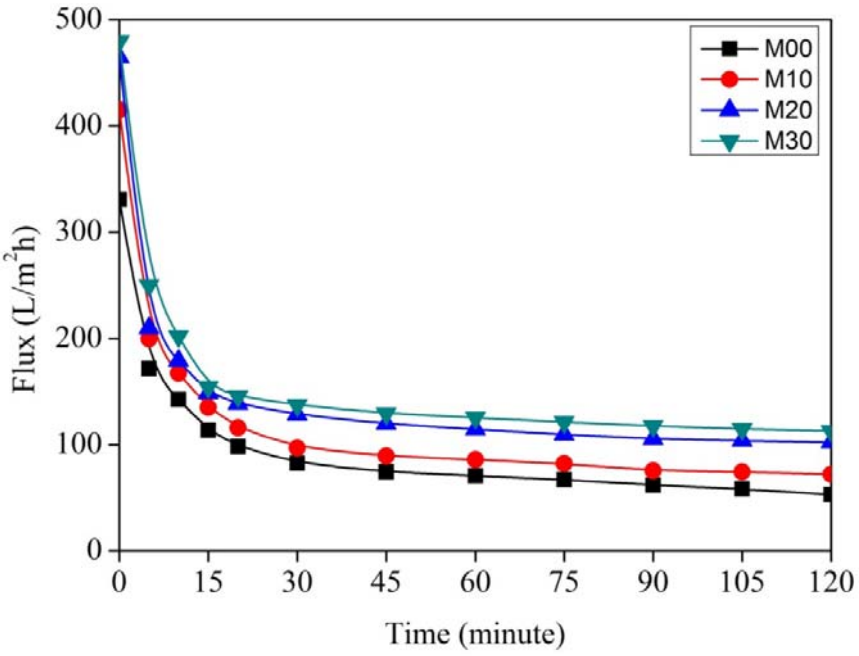

Figure 10a: Flux profile during compaction (at 400 kPa).

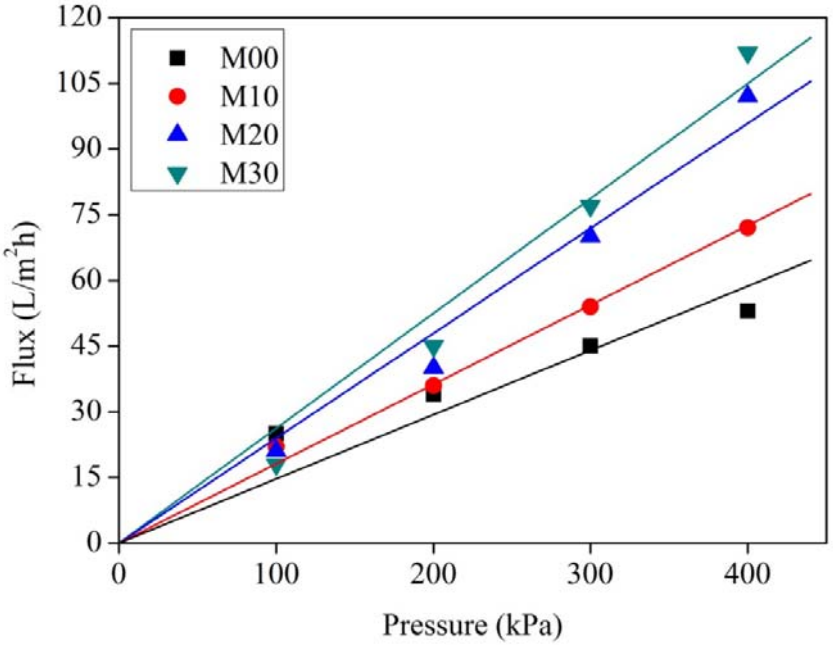

Figure 10b: Pressure dependent flux through different membranes.

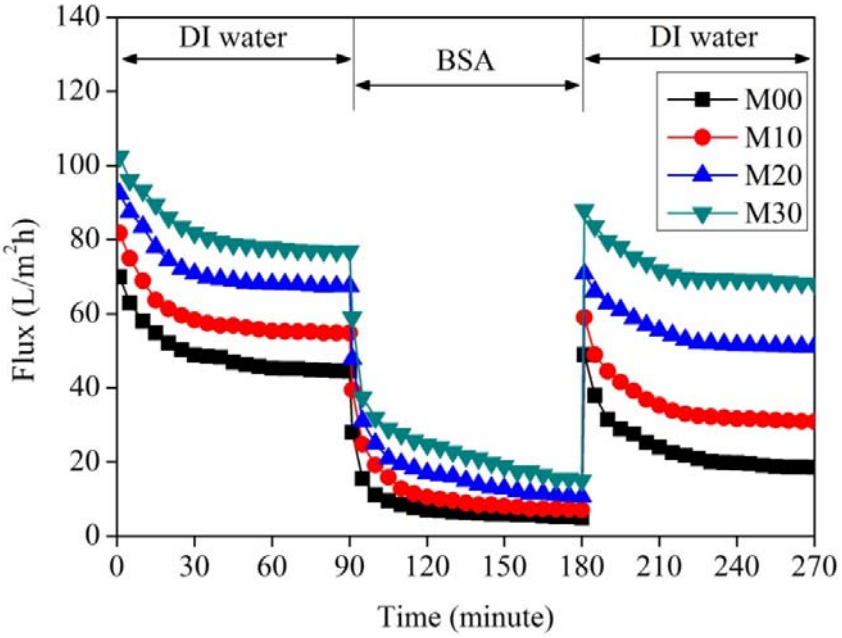

Figure 11: Time dependent flux for prepared membranes for fouling study.

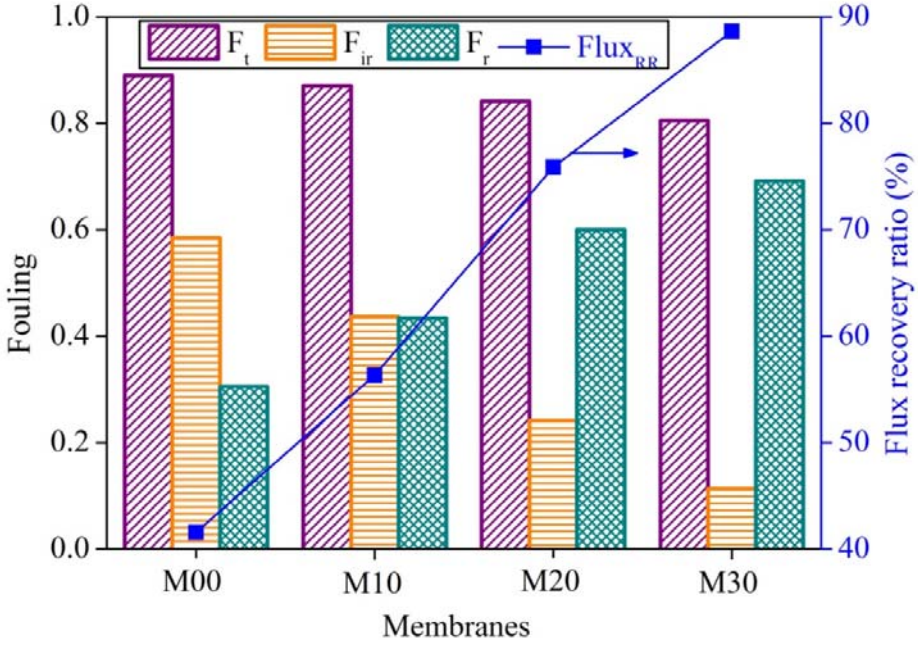

Figure 12: Fouling behaviour and flux recovery ratio of different membranes.

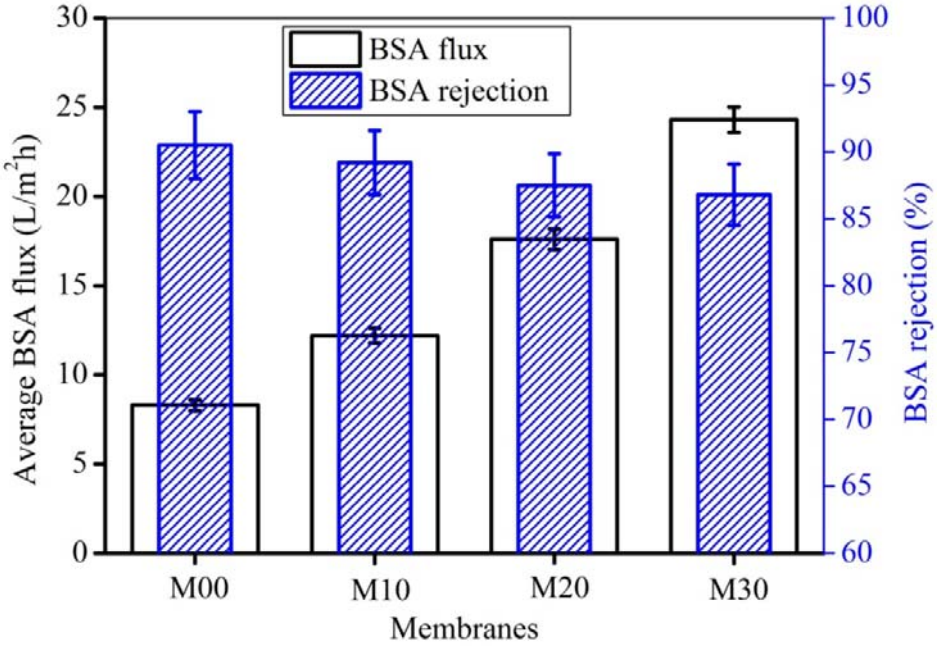

Figure 13: BSA flux and rejection values.

Table 1: Literatures related to nanoparticle additive.

Nanoparticle	Modified/Unmodified	Base polymer	Application	Reference
TiO_2	Modified	PSF	UF (BSA solution)	[16]
TiO_2	Unmodified	PSF	UF (humic acid)	[17]
TiO_2	Unmodified (synthesized)	PVDF	UF (BSA solution)	[18]
ZnO	Unmodified	PSF	UF (oleic acid)	[19]
Boehmite	Unmodified	PES	UF (whey solution)	[20]
SiO_2	Unmodified	PSF	UF (oil in water emulsion)	[21]
ZnO	Unmodified	PES	Dye removal	[22]
Carbon nanotube	Amine functionalized	PES	UF (BSA solution)	[23]
SiO_2	Polymer grafted	PSF	UF (PEG solution)	[24]
$CaCO_3$	Unmodified (synthesized)	PSF	UF (BSA solution)	[25]
Silver	Unmodified	PSF	UF (protein and carbohydrate)	[26]
Silver	Unmodified	PSF	UF (BSA solution)	[27]
Al_2O_3	Unmodified	PES	UF (PEG solution)	[28]
Carbon nanotube	Unmodified (synthesized)	PSF	UF (PEG, PVP and BSA solution)	[29]
Fe_3O_4	Modified	PES	UF (Powder milk solution)	[30]
$Mg(OH)_2$	Unmodified	PVDF	Bacterial solution	[31]

Table 2: Composition and viscosity of different membrane casting solution.

Membranes	**30 % PSF solution in NMP (wt %)**	**10 % CS-PAA solution in NMP (wt %)**	**NMP (wt %)**	**Viscosity $\times 10^2$ (Pa s)**
M00	50	0	50	5.68
M10	50	10	40	6.45
M20	50	20	30	8.05
M30	50	30	20	10.85

Table 3: Some characteristic parameters of fabricated membranes.

Membranes	**C. F.**	**P_m (L/m^2 h kPa)**	**Porosity**	**r_m (nm)**
M00	6.23	0.146	0.785±0.02	7.49±0.18
M10	5.76	0.183	0.77±0.045	8.54±0.44
M20	4.55	0.239	0.765±0.035	9.46±0.44
M30	4.25	0.265	0.78±0.05	10.15±0.5